IEEE Access
Multidisciplinary : Rapid Review : Open Access Journal

Received June 20, 2019, accepted July 7, 2019, date of publication July 10, 2019, date of current version July 26, 2019.

Digital Object Identifier 10.1109/ACCESS.2019.2927864

Design of Linking Matrix in JSCC Scheme Based on Double Protograph LDPC Codes

QIWANG CHEN[1], SHAOHUA HONG[2,3], (Member, IEEE), AND YIFAN CHEN[4,5], (Senior Member, IEEE)

[1]Faculty of Information Science and Engineering, Ningbo University, Ningbo 315000, China
[2]Department of Communication Engineering, Xiamen University, Xiamen 361005, China
[3]Shenzhen Research Institute of Xiamen University, Shenzhen 518057, China
[4]School of Life Science and Technology, University of Electronic Science and Technology of China, Chengdu 610000, China
[5]Faculty of Science and Engineering, University of Waikato, Hamilton 3240, New Zealand

Corresponding author: Shaohua Hong (hongsh@xmu.edu.cn)

This work was supported in part by the National Natural Science Foundation of China under Grant 61671395 and in part by the Guangdong Natural Science Foundation of China under Grant 2018A030313710.

ABSTRACT A joint source channel coding (JSCC) scheme based on source and channel low density parity check (LDPC) codes, which is named as the D-LDPC system, has attracted a lot of attention recently. However, it suffers from a high error-floor. By introducing a linking matrix connecting variable nodes of source LDPC and check nodes of channel LDPC, the error-floor can be lowered effectively. However, the water-fall performance was lost with the increasing of the size of linking matrix. In this paper, a detailed analysis about the impact of this linking matrix on the water-fall region is conducted. Some design principles for the linking matrix are proposed, by which several linking matrices for different source statistics will be designed to improve the water-fall performance from the perspective of both the source and channel LDPC codes. The extrinsic information transfer (EXIT) analysis and numerical simulations will be compared to verify the superiority of the proposed linking matrices.

INDEX TERMS JSCC, linking matrix, source and channel LDPC, water-fall region, EXIT.

I. INTRODUCTION

Low density parity check (LDPC) code employed as channel coding has exhibited performance close to capacity over a binary symmetric memoryless channel [1]. It can also approach Slepian-Wolf limits when used as source coding for a binary source with correlated information [2]. However, the optimal performance of separate source and channel coding can be acquired only when the length of codeword is infinite. A finite-length joint source-channel coding (JSCC) [3], as an alternative scheme, can achieve better performance in practical communication systems because source redundancy is further employed in joint decoding.

A JSCC scheme named as double LDPC (D-LDPC) was proposed in [4], where two LDPC codes were used as source coding and channel coding, respectively. Many efforts have been paid to improve the water-fall performance of the D-LDPC system. A finite-length extrinsic information transfer (EXIT) algorithm [5] was presented to calculate the decoding threshold of the D-LDPC system, where the protograph LDPC was introduced due to its linear complexity of encoding and decoding [6]–[9]. An unequal power allocation strategy using the speciality of non-uniform source was presented in [10]. A re-design of channel protograph LDPC (PLDPC) proposed in [11] lowered the decoding threshold of the D-LDPC system. Several source and channel codes pairs were jointly optimized in [12]. The optimal edge connection between variable nodes (VNs) of channel LDPC and check nodes (CNs) of source LDPC was analayzed in [13]. A window-decoding scheme [14] was proposed for the D-LDPC system based on the concatenated spatially coupled LDPC codes.

On the other hand, D-LDPC system suffered from a high error-floor which limits its application in communication systems. A rate-adaptive family of source PLDPC codes with a lower error-floor level was proposed in [15]. As the error floor was caused by the lost of original source information, a **linking matrix** connecting VNs of source LDPC and CNs of channel LDPC was introduced [16], where more available information was provided for joint decoding. Some improvements in both water-fall and error-floor region were obtained by an information-shorten algorithm [17], but it

The associate editor coordinating the review of this manuscript and approving it for publication was Yan Zhang.

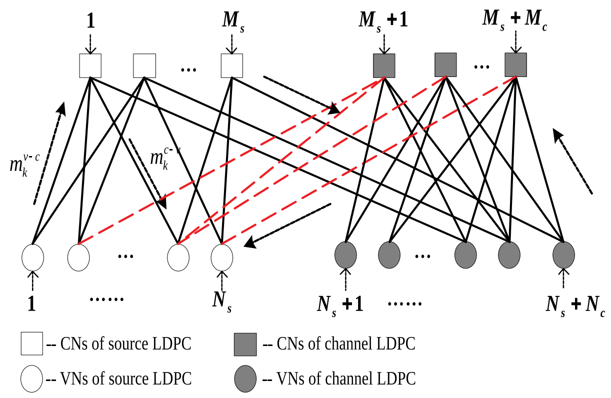

FIGURE 1. The joint tanner graph, where the dash (red) lines represent the edges in the linking matrix H_l.

sacrificed the transmission rate. An adaptive scheme for image transmission in Internet of Things (IoTs) scenarios was proposed [18].

Simple analysis of this linking matrix was presented in [19], which showed its function to lower the error-floor as the number of edges in this linking matrix increases, but it gave rise to the loss of water-fall performance. In addition, both [16] and [19] indicated that the single edge in linking matrix could bring better water-fall performance, which ignored the effectiveness of special source statistics. In this paper, the D-PLDPC system will be considered due to the easy operation and optimization of protograph. A detailed analysis about the linking matrix for the impact on water-fall performance will be conducted. The corresponding protograph of linking matrix will be designed for different source statistics by the aid of the joint protograph EXIT (JPEXIT) algorithm, especially for a high-entropy source. Decoding threshold analysis and numerical simulation will be compared to verify the superiority of the proposed linking matrix.

The detailed contribution of this paper can be concluded as follows;

1) It is found that the linking matrix with multi-edges has better performance in water-fall region than that with single-edges for high-entropy source.
2) Several design principles are proposed to guide the optimization of linking matrix.
3) With the aid of JPEXIT algorithm and differential evolution searching algorithm, some optimized linking matrices are designed for source statistic $p_1 = 0.13$.

The remainder of the letter is organized as follows. Section II presents the model of the D-PLDPC system. In Section III, the motivation, analysis and design algorithm are presented. The simulation results and the comparisons are discussed in Section IV. Section V draws a conclusion.

II. SYSTEM MODEL

A. JOINT PROTOGRAPH

A joint protograph for the D-PLDPC system represented by a base matrix $\boldsymbol{B}_J = [b_{ij}]$ (b_{ij} is a non-negative integer, which is also called "edge") is described as follows,

$$\boldsymbol{B}_J = \left[\begin{array}{c:cc} \boldsymbol{B}_s & 0 & \boldsymbol{I}_B \\ \boldsymbol{B}_l' & & \boldsymbol{B}_c \end{array}\right], \tag{1}$$

where the sizes of source protograph $\boldsymbol{B}_s$, channel protograph $\boldsymbol{B}_c$, linking protograph $\boldsymbol{B}_l'$ and an identity base matrix $\boldsymbol{I_B}$ are $m_s \times n_s$, $m_c \times n_c$, $m_c \times n_s$ and $m_s \times m_s$, respectively. The number of non-zero column vector in $\boldsymbol{B}_l$ is not necessarily n_s, i.e.,

$$\boldsymbol{B}_l' = [\, \boldsymbol{B}_l \;\; \boldsymbol{0} \,], \tag{2}$$

where $\boldsymbol{B}_l$ is with size $m_s \times n_{add}$. The total coderate r_{total} of the D-PLDPC system is given by

$$r_{total} = (n_s/m_s) \times (n_c - m_c)/n_c, \tag{3}$$

The corresponding parity-check matrix $\boldsymbol{H}_J$ can be obtained through the "copy-and-permute" operation implemented by the progressive edge growth (PEG) algorithm [20], which is represented by

$$\boldsymbol{H}_J = \left[\begin{array}{cc:cc} \multicolumn{2}{c:}{\boldsymbol{H}_s} & 0 & \boldsymbol{I}_H \\ \boldsymbol{H}_l & 0 & & \boldsymbol{H}_c \end{array}\right], \tag{4}$$

where $M_s \times N_s$ $\boldsymbol{H}_s$ matrix is the source PLDPC code, $M_c \times N_c$ $\boldsymbol{H}_c$ matrix is the channel PLDPC code, $M_c \times N_{add}$ $\boldsymbol{H}_l$ linking matrix represents the linkage relationship between the VNs of source code and the CNs of channel code and $M_s \times M_s$ $\boldsymbol{I_H}$ is the corresponding identity matrix.

B. ENCODER

At the encoder [19], an original source bits-vector $\boldsymbol{s}$ is generated from a binary independent and identically distributed (i.i.d.) Bernoulli (p_1) source, where p_1 is the probability of "1". The source entropy is calculated by

$$Entropy = -p_1 \log_2 p_1 - (1 - p_1)\log_2(1 - p_1), \tag{5}$$

where the function is monotonically increasing when $0 < p_1 < 0.5$. Thus, high-entropy source following is to represent source with larger p_1.

Then, the source vector is encoded into a compressed bits-vector $\boldsymbol{c}$ by the parity-check matrix $\boldsymbol{H}_s$, i.e.,

$$\boldsymbol{c} = \boldsymbol{s} \cdot \boldsymbol{H}_s^T, \tag{6}$$

where $\{\cdot\}^T$ is the matrix transposition. Next, one part of the original source bits $\boldsymbol{s}'$ and the compressed bits-vector $\boldsymbol{c}$ are integrated into a new bits-vector $[\boldsymbol{s}', \boldsymbol{c}]$ and encoded by the corresponding generate matrix $\boldsymbol{G}_{new}$ of a new parity-check matrix $\boldsymbol{H}_{new} = [\boldsymbol{H}_l | \boldsymbol{H}_c]$, i.e.,

$$[\boldsymbol{s}', \boldsymbol{c}, \boldsymbol{p}] = [\boldsymbol{s}', \boldsymbol{c}] \cdot \boldsymbol{G}_{new} \tag{7}$$

where $\boldsymbol{p}$ is the parity-check bits-vector. $\boldsymbol{s}'$ will be punctured before transmission. The channel is AWGN with noise variance σ_n^2, which is calculated by

$$\sigma_n^2 = 1/(2 \times r_{total} \times Es/N0), \tag{8}$$

where Es is the average energy per original source bit and $N0$ is the average energy of noise.

C. DECODER

Although the encoder is divided into source coding and channel coding, the decoder can be considered as whole. Compared with the belief propagation (BP) in separate decoding [21], the initialization of likelihood log ratio (LLR) values of VNs is different [19].

As shown in Fig. 1, for the VNs set $\{1, 2, \cdots, N_s\}$, the LLR $\boldsymbol{Z}_{sc}$ of the original source bits is calculated by

$$\boldsymbol{Z}_{sc} = \ln\frac{1-p_1}{p_1} \tag{9}$$

For the VNs set $\{N_s+1, \cdots, N_s+N_c\}$, the LLR $\boldsymbol{Z}_{cc}$ of the transmitted bits is calculated by

$$\boldsymbol{Z}_{cc} = \frac{2\boldsymbol{r}}{\sigma_n^2} \tag{10}$$

where binary phase shift keying (BPSK) modulation is performed here and $\boldsymbol{r}$ are received signals. Let $m_k^{v-c}(m_k^{c-v})$ represents the message passed from the v-th VN (c-th CN) to the c-th CN (v-th VN) in the k-th iteration. Then, the messages passed from VNs to CNs are given by

$$m_k^{v-c} = \begin{cases} Z_{sc}^v + \sum\limits_{c'\neq c} m_{k-1}^{c-v}, v = 1, \cdots, N_s \\ \\ Z_{cc}^v + \sum\limits_{c'\neq c} m_{k-1}^{c-v}, v = N_s+1, \cdots, N_s+N_c \end{cases} \tag{11}$$

The messages passed from CNs to VNs are given by

$$m_k^{c-v} = 2\tanh^{-1}\Big(\prod_{v'\neq v}\tanh\big(\frac{m_{k-1}^{v-c}}{2}\big)\Big), \quad c = 1, \cdots, M_s+M_c, \tag{12}$$

where $\tanh(\cdot)$ is the hyperbolic tangent function and $\tanh^{-1}(\cdot)$ is the corresponding inverse function. Lastly, the standard information iteration processing of belief propagation (BP) algorithm between CNs and VNs is implemented to decide the estimated original bits $\hat{\boldsymbol{s}}$.

III. JOINT PROTOGRAPH EXIT ALGORITHM

From a global perspective, the JPEXIT algorithm was proposed in [11] to analysis the decoding threshold of joint protograph. The detailed procedure is presented in the following.

Firstly, five types of mutual information (MI) are defined by

- $I_E^{v-c}(i,j)$: the extrinsic MI from j-th VN to i-th CN
- $I_E^{c-v}(i,j)$: the extrinsic MI from i-th CN to j-th VN
- $I_A^{v-c}(i,j)$: the a prior MI from j-th VN to i-th CN
- $I_A^{c-v}(i,j)$: the a prior MI from i-th CN to j-th VN
- $I_{App}^v(j)$: the MI between a posterior LLR evaluated by j-th VN and the corresponding source bit s_j.

In addition, a function $J(\sigma_n)$ is defined to represent the MI between a binary bit and its corresponding LLR value L_{ch}, given by [1]

$$J(\sigma_{ch}) = 1 - \int_{-\infty}^{\infty} \frac{e^{-(\xi-\sigma_{ch}^2/2)^2/2\sigma_{ch}^2}}{\sqrt{2\pi\sigma_{ch}^2}} \cdot \log_2(1+e^{-\xi})d\xi, \tag{13}$$

where L_{ch} follows the Gaussian distribution with the mean $\sigma_{ch}^2/2$ and the variance σ_{ch}^2.

Finally, the proposed JPEXIT algorithm for DP-LDPC over AWGN is described as follows.

1) The MI update from VNs to CNs

For $i = 1, \cdots, m_s+m_c$ and $j = 1, \cdots, n_s$, if $b_{ij} \neq 0$,

$$I_E^{v-c}(i,j) = J_{Bsc}\Big(\sum_{i'\neq i} b_{i'j}[J^{-1}(I_A^{v-c}(i',j))]^2 + (b_{ij}-1)[J^{-1}(I_A^{v-c}(i,j))]^2, p_1\Big). \tag{14}$$

The function J_{Bsc} is defined as

$$J_{Bsc}(\mu, p_1) = (1-p_1)I(V;\chi^{(1-p_1)}) + p_1 I(V;\chi^{p_1}),$$

where $I(V;\chi)$ is the MI between the VN of the source and χ, $\chi^{(1-p_1)} \sim N(\mu + Z_v^{sc}, 2\mu)$ and $\chi^{p_1} \sim N(\mu - Z_v^{sc}, 2\mu)$ with $Z_v^{sc} = \ln((1-p_v)/p_v)$. If $b_{ij} = 0$, $I_E^{v-c}(i,j) = 0$.

For $i = 1, \cdots, m_s+m_c$ and $j = n_s+1, \cdots, n_s+n_c$, if $b_{ij} \neq 0$,

$$I_E^{v-c}(i,j) = J\Bigg(\sqrt{\sum_{i'\neq i} b_{i'j}[J^{-1}(I_A^{v-c}(i',j))]^2 + (b_{ij}-1)[J^{-1}(I_A^{v-c}(i,j))]^2 + \sigma_{ch}^2(j)}\Bigg). \tag{15}$$

For $i = 1, \cdots, m_s+m_c$ and $j = 1, \cdots, n_s+n_c$

$$I_A^{c-v}(i,j) = I_E^{v-c}(i,j).$$

2) The MI update from CNs to VNs

For $i = 1, \cdots, m_s+m_c$ and $j = 1, \cdots, n_s+n_c$

$$I_E^{c-v}(i,j) = \Bigg(1 - J\sqrt{\Big(\sum_{j'\neq j} b_{ij'}[J^{-1}(1-I_A^{c-v}(i,j'))]^2\Big) + (b_{ij}-1)[J^{-1}(1-I_A^{c-v}(i,j))]^2}\Bigg) \tag{16}$$

and set $I_A^{v-c}(i,j) = I_E^{c-v}(i,j)$

3) The APP-LLR MI evaluation

For $j = 1, \cdots, n_s$

$$I_{App}^v(j) = J_{Bsc}\Big(\sum_i b_{ij}[J^{-1}(I_A^{v-c}(i,j))]^2, p_1\Big), \tag{17}$$

and for $j = n_s+1, \cdots, n_s+n_c$,

$$I_{App}^v(j) = J\Bigg(\sqrt{\sum_i b_{ij}[J^{-1}(I_A^{v-c}(i,j))]^2 + \sigma_{ch}(j)}\Bigg) \tag{18}$$

The iteration procedure is implemented until all $I_{App}^v(j) = 1$ or the iteration maximum is reached.

IV. ANALYSIS AND DESIGN OF LINKING MATRIX

A. MOTIVATION

As analyzed in [16], [19], a non-zero linking matrix can lower the error-floor level, but the performance in the waterfall region will degrade with the increasing of n_{add}. It also indicated that the degree of VNs[1] in $\boldsymbol{B}_l$ made a performance trade-off between the water-fall and error-floor regions. Thus, single-edge[2] in $\boldsymbol{B}_l$ was designed for better water-fall performance.

However, the restriction on the column weight about $\boldsymbol{B}_l$ limits the optimization and neglects the effects from source statistics. For a fixed $\boldsymbol{B}_J$, as the entropy of source increases, source information is harder to be recovered, especially only through the single edge in $\boldsymbol{B}_l$. The loss of information will reduce the speed of convergence and enlarge the decoding threshold. Thus, the column weight in $\boldsymbol{B}_l$ may be larger than 1 for the source with higher-entropy.

B. ANALYSIS

1) REGULAR CHANNEL PROTOGRAPH

In order to verify the conjecture, a joint protograph is given as an example, i.e.,

$$\boldsymbol{B}_{J1} = \left[\begin{array}{c|c} 11101110 & 00001000 \\ 01110111 & 00000100 \\ 10111011 & 00000010 \\ 11011101 & 00000001 \\ \hdashline & 11101110 \\ & 01110111 \\ \boldsymbol{B}_l \ \boldsymbol{0} & 10111011 \\ & 11011101 \end{array}\right], \tag{19}$$

where $\boldsymbol{B}_s$ and $\boldsymbol{B}_c$ are both coderate-1/2 regular protograph with the degree of VNs being 3 and the degree of CNs being 6. Without loss of generality, the n_{add} is 3 and the column vectors are $[0001]^T$, $[0002]^T$ and $[0003]^T$ for the column and row weights being 1, 2 and 3, respectively, so the $\boldsymbol{B}_l^{w1}$, $\boldsymbol{B}_l^{w2}$ and $\boldsymbol{B}_l^{w3}$ are given by

$$\boldsymbol{B}_l^{w1} = \begin{bmatrix} 0 & 0 & 0 \\ 1 & 0 & 0 \\ 0 & 1 & 0 \\ 0 & 0 & 1 \end{bmatrix}, \quad \boldsymbol{B}_l^{w2} = \begin{bmatrix} 0 & 0 & 0 \\ 2 & 0 & 0 \\ 0 & 2 & 0 \\ 0 & 0 & 2 \end{bmatrix},$$
$$\boldsymbol{B}_l^{w3} = \begin{bmatrix} 0 & 0 & 0 \\ 3 & 0 & 0 \\ 0 & 3 & 0 \\ 0 & 0 & 3 \end{bmatrix}, \tag{20}$$

where these edges are at different rows and columns to set up more connections between source and channel protographs, i.e., the rank of their row and column is n_{add}.

As described in Table 1 and Fig. 2, the superiority of $\boldsymbol{B}_l^{w1}$ is a little for a lower-entropy source, but fades away as the entropy increases. In detail, the decoding threshold of $\boldsymbol{B}_J$ with $\boldsymbol{B}_l^{w1}$ is lower than that of $\boldsymbol{B}_l^{w2}$ when $p_1 \leq 0.12$ but higher than that of $\boldsymbol{B}_l^{w2}$ when $p_1 \geq 0.13$. The decoding threshold of $\boldsymbol{B}_J$ with $\boldsymbol{B}_l^{w1}$ has no advantage compared to that of $\boldsymbol{B}_l^{w3}$ when $p_1 \geq 0.14$. The difference between the decoding thresholds of $\boldsymbol{B}_l^{w1}$ and $\boldsymbol{B}_l^{w2}$ becomes larger for a high-entropy source, which is 1.686 dB at $p_1 = 0.17$. Thus, it can be concluded that the column and row weight of $\boldsymbol{B}_l$ can be 1 for low-entropy source but should be larger than 1 for a high-entropy source, and $\boldsymbol{B}_l$ should be optimized for different source entropies.

2) IRREGULAR CHANNEL PROTOGRAPH

In [19], the position of several single-edges in $\boldsymbol{B}_l$ is analyzed according to the degree distribution of source VNs, where connecting the maximum degree has a better decoding threshold. However, the analysis does not consider the effects due to the construction of channel CNs. In order to shed some light on this problem, a joint protograph with a 4×8 irregular protograph [15] and a 4×8 regular protograph[3] is given by

$$\boldsymbol{B}_{J2} = \left[\begin{array}{cccccccc|cccccccc} 1 & 1 & 1 & 0 & 1 & 1 & 1 & 0 & 0 & 0 & 0 & 0 & 1 & 0 & 0 & 0 \\ 0 & 1 & 1 & 1 & 0 & 1 & 1 & 1 & 0 & 0 & 0 & 0 & 0 & 1 & 0 & 0 \\ 1 & 0 & 1 & 1 & 1 & 0 & 1 & 1 & 0 & 0 & 0 & 0 & 0 & 0 & 1 & 0 \\ 1 & 1 & 0 & 1 & 1 & 1 & 0 & 1 & 0 & 0 & 0 & 0 & 0 & 0 & 0 & 1 \\ \hdashline b_{11} & b_{12} & b_{13} & 0 & 0 & 0 & 0 & 0 & 1 & 0 & 0 & 0 & 3 & 3 & 0 & 0 \\ b_{21} & b_{22} & b_{23} & 0 & 0 & 0 & 0 & 0 & 0 & 1 & 0 & 0 & 2 & 3 & 0 & 1 \\ b_{31} & b_{32} & b_{33} & 0 & 0 & 0 & 0 & 0 & 0 & 0 & 1 & 1 & 3 & 2 & 1 & 2 \\ b_{41} & b_{42} & b_{43} & 0 & 0 & 0 & 0 & 0 & 2 & 2 & 2 & 1 & 0 & 0 & 2 & 0 \end{array}\right], \tag{21}$$

where the degree of CNs channel protograph is {7,7,10,9} and $n_{add} = 3$ is assumed without loss of generality. $b_{11} = 1$ corresponds to connecting the CNs with degree being 7, $b_{22} = 1$ for 7, $b_{32} = 1$ for 10 and $b_{43} = 1$ for 9 (any other b_{ij} is 0).

The decoding threshold of the joint protograph $\boldsymbol{B}_{J2}$ with different $\boldsymbol{B}_l^{w1}$ at different p_1 are calculated as shown in Table II. By comparing the two cases at $p_1 = 0.06$ with low-entropy and $p_1 = 0.13$ with high-entropy, the lowest decoding thresholds is {7,10,9} at $p_1 = 0.06$ with the maximum average degree of channel CNs but it is {7,7,9} at $p_1 = 0.11$ with the minimum one. By contrast, the decoding thresholds at $p_1 = 0.13, 0.14, 0.15$ are unusual. Thus, the design for $\boldsymbol{B}_l$ should take into account source entropy and the construction of irregular channel protograph.

Follow the aforementioned analysis, the design of $\boldsymbol{B}_l$ is obviously related to the construction of irregular source protograph, which is not analyzed here and will be designed in the next subsection.

C. DESIGN ALGORITHM

Relative to a high-entropy source, the biggest difference of designing $\boldsymbol{B}_l$ for a low-entropy source is to minimize the usage of single-edges to make the row and column weights. Meanwhile, using single-edge makes the design of $\boldsymbol{B}_l$ simple, which has been performed in the analysis above. Thus,

[1]The degree of VNs is the sum of elements in a column, which is also called the column weight.

[2]The element being 1 is called as single-edge and being b_l^{max} ($b_l^{max} \geq 2$) is multi-edge.

[3]The reason using regular source protograph here is to exclude the effects from the VNs of source protograph which has been analyzed in [19] for the analysis.

TABLE 1. The decoding threshold $Es/N0_{th}$ of joint protograph B_{J1} with different B_l at different source statistic.

p_1	0.06	0.07	0.08	0.09	0.1	0.11	0.12	0.13	0.14	0.15	0.16	0.17
Entropy	0.3274	0.3659	0.4022	0.4365	0.4690	0.4999	0.5294	0.5574	0.5842	0.6098	0.6343	0.6577
B_l^{w1}	**-2.612**	**-2.184**	**-1.768**	**-1.382**	**-0.990**	**-0.625**	**-0.217**	0.213	0.720	1.288	2.104	3.066
B_l^{w2}	-2.548	-2.072	-1.618	-1.212	-0.822	-0.488	-0.130	**0.174**	**0.497**	**0.792**	**1.091**	**1.380**
B_l^{w3}	-2.490	-1.981	-1.548	-1.108	-0.679	-0.344	-0.006	0.374	0.647	0.912	1.206	1.445

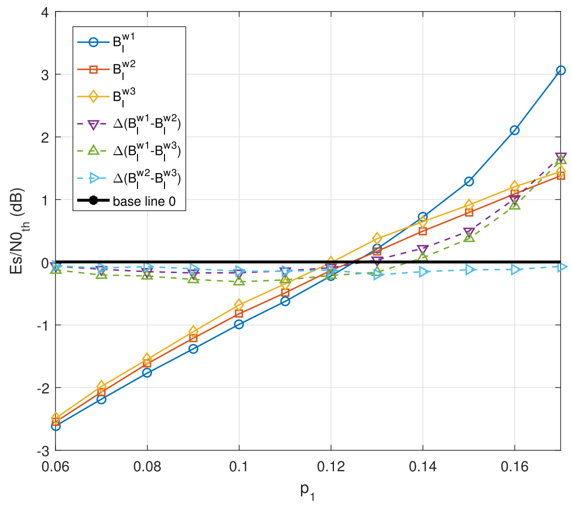

FIGURE 2. The difference value of decoding threshold among B_l^{w1}, B_l^{w2} and B_l^{w3} from source statistic $p_1 = 0.06$ to 0.17 .

TABLE 2. The decoding threshold $Es/N0_{th}$ of joint protograph B_{J2} with different B_l^{w1} at $p_1 = 0.06, 0.07, 0.08, 0.11, 0.13, 0.14$ and 0.15.

p_1	$b_{11}b_{22}b_{32}$	$b_{11}b_{22}b_{43}$	$b_{11}b_{32}b_{43}$	$b_{22}b_{32}b_{43}$
0.06	-3.093	-3.120	-3.182	**-3.212**
0.07	-2.621	-2.653	-2.739	**-2.792**
0.08	-2.220	-2.207	-2.366	**-2.399**
0.11	-1.131	**-1.143**	-0.985	-0.733
0.13	**-0.368**	-0.273	0.195	0.562
0.14	**0.030**	0.209	0.886	1.223
0.15	**0.491**	0.813	1.629	1.975

the design algorithm is mainly focused on the high-entropy source.

Several design principles for a high-entropy source can be concluded as follows,

1) The kind of multi-edge ($b_l^{max} \geq 2$) is suggested in $\boldsymbol{B}_l$;
2) The number of row weight and column weight no less w ($w \geq 2$) is no less than $\min(m_s, n_{add})$;
3) The row and column rank is no less than $\min(m_s, n_{add})$.

Differential evolution (DE) algorithm [22] can be used to search for $\boldsymbol{B}_l$. The decoding threshold $Es/N0_{th}$ calculated by the JPEXIT algorithm is used as the cost function in differential evolution, i.e.,

$$\begin{aligned} &\min_{\boldsymbol{B}_l} \quad \Phi(\boldsymbol{B}_J) \\ &\text{s.t.} \quad \Omega(\boldsymbol{B}_l) = 1 \end{aligned} \tag{22}$$

where $\Phi(\boldsymbol{B}_J)$ returns the decoding threshold $Es/N0_{th}$ and $\Omega(\cdot) = 1$ represents $\Omega(\boldsymbol{B}_l)$ satisfying the required conditions; otherwise $\Omega(\cdot) = 0$. The procedures of DE algorithm are given as follows

- *GIVEN*: an initial source protograph $\boldsymbol{B}_l$ with fixed column indices F_l and an given $\boldsymbol{B}_s$ and $\boldsymbol{B}_c$, i.e., (1); the number of candidate matrix Ψ_c; the number of generations Ψ_g; the crossover probability p_c.
- *REQUIRED CONDITIONS*: (i) The row and column rank is no less than $\min(m_s, n_{add})$; (ii) the number of row weight and column weight is at least w; (iii) the maximum value of the left elements in $\boldsymbol{B}_l$ is b_l^{max};

1) *INITIALIZATION*: Set $\boldsymbol{B}_l^{1(0)}$ to be $\boldsymbol{B}_l^{ini}$. For $2 \leq \varphi_c \leq \Psi_c$, $\boldsymbol{B}_l^{\varphi_c(0)}$ is generated by replacing the elements in $\boldsymbol{B}_l^{1(0)}$ except for the fixed columns with random integer values from 0 to b_{max}. The process is repeated until every $\boldsymbol{B}_l^{\varphi_c(0)}$ satisfies required conditions.
2) *MUTATION*: For $1 \leq \varphi_c \leq \Psi_c$, mutation matrix $\boldsymbol{M}_s^{\varphi_c(\varphi_g)}$ of a given generation φ_g is given by
$$\boldsymbol{M}_l^{\varphi_c(\varphi_g)} = \Theta\Big(\boldsymbol{B}_l^{r_1(\varphi_g)} + 0.5(\boldsymbol{B}_l^{r_2(\varphi_g)} - \boldsymbol{B}_l^{r_3(\varphi_g)})\Big)$$
where r_1, r_2 and r_3 are randomly selected in the scope $[1, \Psi_c]$, and $\Theta(\boldsymbol{B})$ is an operation to replace each element in $\boldsymbol{B}$ with an integer closest to its absolute value.
3) *CROSSOVER*: For $1 \leq \varphi_c \leq \Psi_c$, (i, j)-th of a candidate matrix $\boldsymbol{N}_l^{\varphi_c(\varphi_g)}$ is set as the (i, j)-th element of $\boldsymbol{M}_l^{\varphi_c(\varphi_g)}$ with probability p_c, or as the (i, j)-th element of $\boldsymbol{B}_l^{\varphi_c(\varphi_g)}$ with probability $(1 - p_c)$.
4) *SELECTION*: For $1 \leq \varphi_c \leq \Psi_c$, protograph of generation $g + 1$ are set according to the rule, if $\Phi(\boldsymbol{B}_{J_N})\Omega(\boldsymbol{N}_l^{\varphi_c(\varphi_g)}) > \Phi(\boldsymbol{B}_{J_B})$, $\boldsymbol{B}_l^{\varphi_c(\varphi_g+1)} = \boldsymbol{N}_l^{\varphi_c(\varphi_g)}$; otherwise, $\boldsymbol{B}_l^{\varphi_c(\varphi_g+1)} = \boldsymbol{B}_l^{\varphi_c(\varphi_g)}$. where

$$\begin{aligned} \boldsymbol{B}_{J_N} &= \left[\begin{array}{cc:cc} \boldsymbol{B}_s & & 0 & \boldsymbol{I}_B \\ \boldsymbol{N}_l^{\varphi_c(\varphi_g)} & 0 & & \boldsymbol{B}_c \end{array}\right], \\ \boldsymbol{B}_{J_B} &= \left[\begin{array}{cc:cc} \boldsymbol{B}_s & & 0 & \boldsymbol{I}_B \\ \boldsymbol{B}_l^{\varphi_c(\varphi_g)} & 0 & & \boldsymbol{B}_c \end{array}\right] \end{aligned} \tag{23}$$

5) *TERMINATION*: Steps 2)-4) are excuted for Ψ_g generations and the protograph with the lowest channel decoding threshold $Es/N0_{th}$ is chose as the solution.

Example-1: The optimization for (21) at $p_1 = 0.13$ is taken as an example, where $m_s = 4$, $n_{add} = 3$, $F_l = \{4, 5, 6, 7, 8\}$, $p_c = 0.88$, $\Psi_c = 3000$ and $\Psi_g = 1000$. The empirical value $w = 2$ is taken to make the performance free of error floor and achieve a low decoding threshold, and $b_l^{max} = 2$ is assumed to reduce the searching space. By applying the searching algorithm, the optimized $\boldsymbol{B}_l^{opt-1}$ can be obtained,

$$\boldsymbol{B}_l^{opt-1} = \begin{bmatrix} 2 & 0 & 0 \\ 0 & 1 & 0 \\ 1 & 1 & 0 \\ 1 & 0 & 2 \end{bmatrix}, \tag{24}$$

where $\boldsymbol{B}_{J2}$ combined with $\boldsymbol{B}_l^{opt-1}$ is called $\boldsymbol{B}_{J2}^{opt-1}$ with decoding threshold being -0.451dB at $p_1 = 0.13$.

Example-2: Different from the case $\boldsymbol{B}_{J2}$ with a regular source protograph, a joint protograph with an irregular source protograph [15] and anther irregular channel protograph [15] is taken as an example, i.e.,

$$\boldsymbol{B}_{J3} = \left[\begin{array}{cccccccc:cccccccc} 3 & 1 & 0 & 2 & 1 & 1 & 0 & 0 & 0 & 0 & 0 & 0 & 1 & 0 & 0 & 0 \\ 2 & 1 & 1 & 3 & 0 & 0 & 1 & 0 & 0 & 0 & 0 & 0 & 0 & 1 & 0 & 0 \\ 3 & 0 & 0 & 3 & 0 & 0 & 0 & 1 & 0 & 0 & 0 & 0 & 0 & 0 & 1 & 0 \\ 3 & 1 & 2 & 0 & 2 & 1 & 1 & 1 & 0 & 0 & 0 & 0 & 0 & 0 & 0 & 1 \\ \hdashline b_{11} & b_{12} & b_{13} & 0 & 0 & 0 & 0 & 0 & 3 & 2 & 2 & 1 & 0 & 1 & 0 & 0 \\ b_{21} & b_{22} & b_{23} & 0 & 0 & 0 & 0 & 0 & 3 & 3 & 0 & 0 & 0 & 0 & 1 & 0 \\ b_{31} & b_{32} & b_{33} & 0 & 0 & 0 & 0 & 0 & 3 & 2 & 1 & 0 & 1 & 0 & 0 & 1 \\ b_{41} & b_{42} & b_{43} & 0 & 0 & 0 & 0 & 0 & 2 & 2 & 0 & 2 & 2 & 1 & 1 & 1 \end{array}\right], \tag{25}$$

where the fixed parameters are the same in **Example-1**. The $\boldsymbol{B}_l^{opt-2}$ satisfying our design principles is obtained by using the differential evolution algorithm, i.e.,

$$\boldsymbol{B}_l^{opt-2} = \begin{bmatrix} 0 & 2 & 0 \\ 1 & 0 & 0 \\ 2 & 0 & 0 \\ 1 & 0 & 2 \end{bmatrix}, \tag{26}$$

where $\boldsymbol{B}_{J3}$ combined with $\boldsymbol{B}_l^{opt-2}$ is called $\boldsymbol{B}_{J3}^{opt-1}$ with decoding threshold being -0.731dB at $p_1 = 0.13$.

V. SIMULATION RESULTS

In order to verify the analysis and optimization of linking matrix, the bit error rate (BER) performance is simulated. The length of the original source bits-vector is 3200 and the total coderate r_{total} is 1.0. The maximum iteration number of BP algorithm is 100. Source statistics $p_1 = 0.06$ and $p_1 = 0.13$ respectively indicate the examples of low-entropy and high-entropy sources.

In order to explain the importance of the design principles-2) and 3), two counter-examples are compared. One $\boldsymbol{B}_l$ against principle- 3) and another $\boldsymbol{B}_l$ against principle-2) are given as follows,

$$\boldsymbol{B}_l^{opt-3} = \begin{bmatrix} 2 & 0 & 0 \\ 2 & 0 & 0 \\ 2 & 0 & 0 \\ 0 & 2 & 2 \end{bmatrix}, \quad \boldsymbol{B}_l^{opt-4} = \begin{bmatrix} 1 & 1 & 0 \\ 1 & 0 & 0 \\ 1 & 0 & 0 \\ 0 & 1 & 2 \end{bmatrix}, \tag{27}$$

where the row and column rank of $\boldsymbol{B}_l^{opt-3}$ is 2, which is less than $n_{add} = 3$, and the number of row weight (≥ 2) is 2, which is less than $n_{add} = 3$. The $\boldsymbol{B}_{J3}$ combined with $\boldsymbol{B}_l^{opt-3}$ is called $\boldsymbol{B}_{J3}^{bad-1}$ with decoding threshold being -0.812dB at $p_1 = 0.13$ and $\boldsymbol{B}_{J3}$ combined with $\boldsymbol{B}_l^{opt-4}$ is called $\boldsymbol{B}_{J3}^{bad-2}$ with decoding threshold being -0.827dB at $p_1 = 0.13$. In addition, $\boldsymbol{B}_{J1}^{w1}$ is the matrix $\boldsymbol{B}_{J1}$ combined with $\boldsymbol{B}_l^{w1}$, $\boldsymbol{B}_{J1}^{w2}$ is the matrix $\boldsymbol{B}_{J2}$ combined with $\boldsymbol{B}_l^{w2}$, $\boldsymbol{B}_{J1}^{w3}$ is the matrix $\boldsymbol{B}_{J1}$ combined with $\boldsymbol{B}_l^{w3}$, $\boldsymbol{B}_{J2}^{w1-worst}$ is the matrix $\boldsymbol{B}_{J2}$ combined with $\boldsymbol{B}_l^{w1}$ of $b_{11} = b_{22} = b_{32} = 1$ and $\boldsymbol{B}_{J2}^{w1-best}$ is the matrix $\boldsymbol{B}_{J2}$ combined with $\boldsymbol{B}_l^{w1}$ of $b_{11} = b_{32} = b_{43} = 1$.

A. LOW-ENTROPY SOURCE OF $P_1 = 0.06$

The BER performance of different D-PLDPC codes at $p_1 = 0.06$ is shown in Fig.3. By comparing the BER performance of $\boldsymbol{B}_{J1}^{w1}$, $\boldsymbol{B}_{J1}^{w2}$ and $\boldsymbol{B}_{J1}^{w3}$, it is verified that the BER performance becomes worse as the row and column weight for low-entropy source increases for a low-entropy source, which is in line with the analysis of decoding threshold. The BER performance of D-PLDPC codes with an irregular channel protograph is better than a regular channel protograph. Compared with $\boldsymbol{B}_{J2}^{w1-worst}$, the BER performance of $\boldsymbol{B}_{J2}^{w1-best}$ has a 0.2 dB coding gain at the 1×10^{-6} BER level, which is in line with the analysis of decoding threshold. This coding gain verifies the superiority of the matrix $\boldsymbol{B}_{J1}^{w1}$ with the best connection relationship.

B. HIGH-ENTROPY SOURCE OF $P_1 = 0.13$

The BER performance of different D-PLDPC codes at $p_1 = 0.13$ is shown in Fig.4. Different from the case with low-entropy source, the decoding threshold of $\boldsymbol{B}_{J1}^{w2}$ has only a 0.039 dB compared with $\boldsymbol{B}_{J1}^{w1}$, but the BER performance of $\boldsymbol{B}_{J1}^{w2}$ is improved by 1.0 dB at the 1.0×10^{-5} BER level. The reason is that the original source information is harder to be recovered for high-entropy through $\boldsymbol{B}_l^{w1}$, where the row and column weight is only 1. By contrast, the matrix $\boldsymbol{B}_l^{w2}$ sets up more connections between source and channel LDPC codes, which lower the level of error floor. Thus, the coding gain becomes larger in the high $Es/N0$ region.

Compared with $\boldsymbol{B}_{J1}^{w2}$, the BER performance of $\boldsymbol{B}_{J2}^{opt}$ and $\boldsymbol{B}_{J3}^{opt}$ has 0.5 dB and 0.85 dB coding gains at the 1.0×10^{-6} BER level, which is in line with the decoding analysis. This coding gain verifies the superiority of the optimized $\boldsymbol{B}_{J2}^{opt}$ and $\boldsymbol{B}_{J3}^{opt}$.

Compared with $\boldsymbol{B}_{J3}^{opt}$, the decoding thresholds of $\boldsymbol{B}_{J3}^{bad-1}$ and $\boldsymbol{B}_{J3}^{bad-2}$ are improved by 0.081 dB and 0.096 dB coding gain, but the BER performance is not so. Firstly, the BER per-

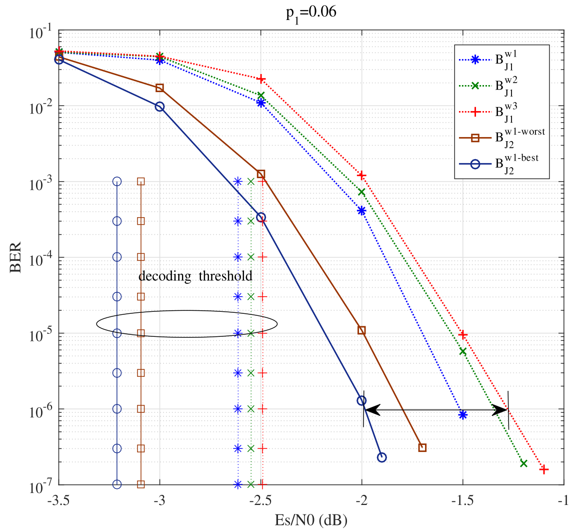

FIGURE 3. The BER performance of different DP-LDPC codes at $p_1 = 0.06$, where the decoding threshold from left to right is −3.212 dB, −3.093 dB, −2.612 dB, −2.548 dB and −2.490 dB.

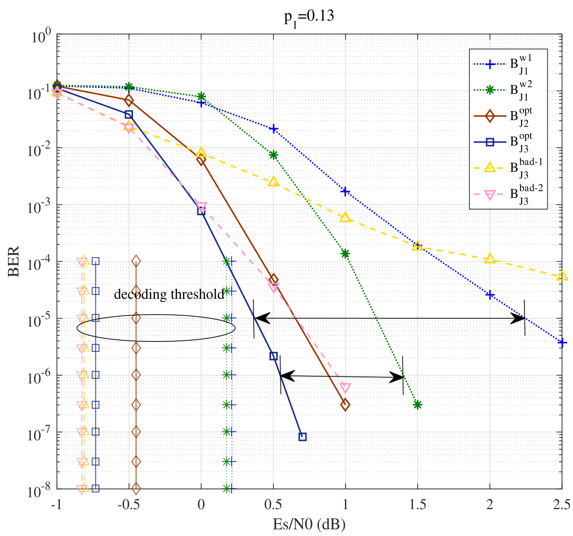

FIGURE 4. The BER performance of different DP-LDPC codes at $p_1 = 0.13$, where the decoding threshold from left to right is −0.827 dB, −0.812 dB, −0.731 dB, −0.451 dB, 0.174 dB and 0.213 dB.

formance of $\boldsymbol{B}_{J3}^{bad-1}$ and $\boldsymbol{B}_{J3}^{bad-2}$ has slight superiority in the $Es/N0$ region from -1.0 dB to -0.5 dB. But, the BER performance of $\boldsymbol{B}_{J3}^{bad-2}$ is worse than that of $\boldsymbol{B}_{J3}^{opt}$ after -0.5 dB and even worse than that of $\boldsymbol{B}_{J2}^{opt}$ after 1 dB, because the number of row weight(≥ 2) is less than that of $\boldsymbol{B}_{J2}^{opt}$ and $\boldsymbol{B}_{J3}^{opt}$ in $\boldsymbol{B}_l$, which results in the loss of original source information. Meanwhile, the BER performance of $\boldsymbol{B}_{J3}^{bad-1}$ has a significant error floor, which illustrates the importance of the construction satisfying principle 3).

In summary, the comparisons of BER performance verify the validity of the design principles for $\boldsymbol{B}_l$. These design principles should be adjusted appropriately according to practical conditions, including source entropy and transmission coderate.

VI. CONCLUSION

In this paper, the analysis for linking matrix connecting VNs of source codes and CNs of channel codes has been performed in the D-PLDPC system. It has been found that the decoding threshold of multi-edges in linking matrix is better that of single-edge for a high-entropy source. In addition, the optimal connectivity of linking matrix is also different between the cases of low-entropy and high-entropy sources. Thus, some design principles for linking matrix have been proposed, by which some optimized examples and counter-examples have been designed. By comparing the decoding threshold and BER performance, the superiority of the optimized linking matrix is verified, e.g., the maximum coding gain has reached up to 1.9 dB at $p_1 = 0.13$.

This letter is mainly focused on the improvement of the water-fall region by designing a suitable linking matrix, especially for a high-entropy source. In future, the improvement of the error-floor region for sources with a much higher entropy will be studied.

REFERENCES

[1] J. Chen and M. P. C. Fossorier, "Near optimum universal belief propagation based decoding of low-density parity check codes," *IEEE Trans. Commun.*, vol. 50, no. 3, pp. 406–414, Mar. 2002.
[2] A. D. Liveris, Z. Xiong, and C. N. Georghiades, "Compression of binary sources with side information at the decoder using LDPC codes," *IEEE Commun. Lett.*, vol. 6, no. 10, pp. 440–442, Oct. 2002.
[3] I. E. Bocharova, A. G. Fàbregas, B. D. Kudryashov, A. Martinez, A. T. Campo, and G. Vazquez-Vilar, "Source-channel coding with multiple classes," in *Proc. IEEE Int. Symp. Inf. Theory*, Honolulu, HI, USA, Jun./Jul. 2014, pp. 1514–1518.
[4] M. Fresia, F. Perez-Cruz, H. V. Poor, and S. Verdu, "Joint source and channel coding," *IEEE Signal Process. Mag.*, vol. 27, no. 6, pp. 104–113, Nov. 2010.
[5] H. Wu, L. Wang, S. Hong, and J. He, "Performance of joint source-channel coding based on protograph LDPC codes over Rayleigh fading channels," *IEEE Commun. Lett.*, vol. 18, no. 4, pp. 652–655, Apr. 2014.
[6] Y. Fang, G. Bi, Y. L. Guan, and F. C. M. Lau, "A survey on protograph LDPC codes and their applications," *IEEE Commun. Surveys Tuts.*, vol. 17, no. 4, pp. 1989–2016, 4th Quart., 2015.
[7] Y. Fang, S. C. Liew, and T. Wang, "Design of distributed protograph LDPC codes for multi-relay coded-cooperative networks," *IEEE Trans. Wireless Commun.*, vol. 16, no. 11, pp. 7235–7251, Nov. 2017.
[8] W. Sułek, "Protograph based low-density parity-check codes design with mixed integer linear programming," *IEEE Access*, vol. 7, pp. 1424–1438, 2019.
[9] Z. Yang, Y. Fang, G. Han, G. Cai, and F. C. M. Lau, "Design and analysis of punctured terminated spatially coupled protograph LDPC codes with small coupling lengths," *IEEE Access*, vol. 6, pp. 36723–36731, 2018.
[10] J. He, Y. Li, G. Wu, S. Qian, Q. Xue, and T. Matsumoto, "Performance improvement of joint source-channel coding with unequal power allocation," *IEEE Wireless Commun. Lett.*, vol. 6, no. 5, pp. 582–585, Oct. 2017.
[11] Q. Chen, L. Wang, S. Hong, and Z. Xiong, "Performance improvement of JSCC scheme through redesigning channel code," *IEEE Commun. Lett.*, vol. 20, no. 6, pp. 1088–1091, Jun. 2016.
[12] C. Chen, L. Wang, and F. C. M. Lau, "Joint optimization of protograph LDPC code pair for joint source and channel coding," *IEEE Trans. Commun.*, vol. 66, no. 8, pp. 3255–3267, Aug. 2018.
[13] S. Liu, C. Chen, L. Wang, and S. Hong, "Edge connection optimization for JSCC system based on DP-LDPC codes," *IEEE Wireless Commun. Lett.*, to be published. doi: 10.1109/LWC.2019.2903442.
[14] A. Golmohammadi and D. Mitchell, "Concatenated spatially coupled LDPC codes for joint source-channel coding," in *Proc. IEEE Int. Symp. Inf. Theory (ISIT)*, Jun. 2018, pp. 631–635.
[15] C. Chen, L. Wang, and S. Liu, "The design of protograph LDPC codes as source codes in a JSCC system," *IEEE Commun. Lett.*, vol. 22, no. 4, pp. 672–675, Apr. 2018.

[16] H. V. B. Neto and W. Henkel, "Multi-edge optimization of low-density parity-check codes for joint source-channel coding," in *Proc. 9th Int. ITG Conf. Syst., Commun. Coding*, Munich, Germany, Jan. 2013, pp. 1–6.

[17] H. V. B. Neto and W. Henkel, "Information shortening for joint source-channel coding schemes based on low-density parity-check codes," in *Proc. 8th Int. Symp. Turbo Codes Iterative Inf. Process. (ISTC)*, Aug. 2014, pp. 122–126.

[18] L. Deng, Z. Shi, O. Li, and J. Ji, "Joint coding and adaptive image transmission scheme based on DP-LDPC codes for IoT scenarios," *IEEE Access*, vol. 7, pp. 18437–18449, 2019.

[19] S. Hong, Q. Chen, and L. Wang, "Performance analysis and optimisation for edge connection of JSCC system based on double protograph LDPC codes," *IET Commun.*, vol. 12, no. 2, pp. 214–219, Jan. 2018.

[20] X.-Y. Hu, E. Eleftheriou, and D. M. Arnold, "Regular and irregular progressive edge-growth tanner graphs," *IEEE Trans. Inf. Theory*, vol. 51, no. 1, pp. 386–398, Jan. 2005.

[21] D. Divsalar, S. Dolinar, C. R. Jones, and K. Andrews, "Capacity-approaching protograph codes," *IEEE J. Sel. Areas Commun.*, vol. 27, no. 6, pp. 876–888, Aug. 2009.

[22] S. Das and P. N. Suganthan, "Differential evolution: A survey of the state-of-the-art," *IEEE Trans. Evol. Comput.*, vol. 15, no. 1, pp. 4–31, Feb. 2011.

QIWANG CHEN received the B.Sc. degree in electronic science and technology from Huaqiao University, Xiamen, China, in 2012, and the Ph.D. degree in communication engineering from Xiamen University, Xiamen, China, in 2018. He was a Visiting Ph.D. student with the Faculty of Engineering, Monash University, Australia. He is currently a Lecturer with the School of Information Science and Engineering, Ningbo University, Ningbo China. His primary research interests include information theory and coding, joint source-channel coding, chaos communication, and the Internet of Things.

SHAOHUA HONG (M'12) received the B.Sc. degree in electronics and information engineering from Zhejiang University, Hangzhou, China, in 2005, and the Ph.D. degree in electronics science and technology from Zhejiang University, Hangzhou, China, in 2010.

He is currently an Associate Processor with the Department of Information and Communication Engineering, Xiamen University, Xiamen, China. His research interests include joint source and channel coding, wireless communication, and image processing.

Dr. Hong serves as an Editor for KSII Transactions on Internet and Information Systems from 2015.

YIFAN CHEN is the Dean of School of Life Science and Technology with the University of Electronic Science and Technology of China. His current research focuses on electromagnetism-oriented biomedicine. He has served as the Coordinator, Working Group Leader, and Advisory Committee Member for several long-term, large-scale European FP7, and H2020 research projects. He is the Vice Chair of the IEEE ComSoc Technical Committee for Molecular, Biological, and Multi-Scale Communications, and has served as the General Chair and TPC Chair for several premier IEEE conferences such as ICC, ICCE-China, ICCC, ICCS, APCAP, APEMC, EDAPS, etc. He is a Fellow of IET.